

Exact results for one-dimensional disordered bosons with strong repulsion

A. De Martino,¹ M. Thorwart,¹ R. Egger,¹ and R. Graham²

¹Institut für Theoretische Physik, Heinrich-Heine-Universität, D-40225 Düsseldorf, Germany

²Fachbereich Physik, Universität Duisburg-Essen, D-45117 Essen, Germany

(Dated: February 2, 2008)

We study one-dimensional disordered bosons with strong repulsive interactions. A Bose-Fermi mapping expresses this problem in terms of non-interacting Anderson-localized fermions, whereby known results for the distribution function of the local density of states, the spectral statistics, and density-density correlations can be transferred to this new domain of applicability. We show that disorder destroys bosonic quasi-long-range order by calculating the momentum distribution, and comment on the experimental observability of these predictions in ultracold atomic gases.

PACS numbers: 03.75.-b, 05.30.Jp

The properties of interacting bosons have recently attracted considerable attention due to the unprecedented control and tunability achieved in ultracold atomic gases. For instance, by using optical lattices, the predicted quantum phase transition from a superfluid state to a Mott insulator [1, 2] has been experimentally observed [3]. Current interest is also directed towards disordered systems, where disorder can be generated by using laser speckle patterns [4], additional incommensurate optical lattice potentials [5, 6], or via atom-surface interactions in micro-chip confined atomic gases [7]. It thus appears feasible to experimentally study dirty bosons under controlled conditions, in contrast to earlier realizations using granular superconductors or Helium-4 in porous media. Unfortunately, the theory of disordered interacting bosons is difficult, and no exact solutions are known apart from numerical or approximate results [1, 8, 9, 10, 11, 12], even in the one-dimensional (1D) limit [13, 14].

In this paper, we show that for strong repulsive interactions, the dirty boson problem in 1D is exactly solvable via a Bose-Fermi mapping discussed before in the clean limit of a Tonks-Girardeau gas [15, 16, 17, 18, 19, 20]. The mapping establishes a connection to non-interacting disordered fermions, allowing to directly apply many results previously obtained on Anderson localization in 1D, and greatly simplifying the computation of other quantities like the momentum distribution. Our predictions can be checked using state-of-the-art experiments. Detailed conditions for the 1D regime have been specified in Refs. [21, 22], and the 1D Tonks-Girardeau regime has recently been achieved [23, 24], see also Refs. [25, 26].

The Bose-Fermi mapping can be established most directly by starting from a lattice description of hard-core bosons, the Bose-Hubbard model [1], which applies immediately to optical-lattice experiments upon expanding the Bose field operator in the Wannier state basis [2]. Considering spinless bosons on a 1D lattice with spacing a , with Bose annihilation operator b_l at site l , the Hamiltonian is

$$H = \sum_l \left(-J_l [b_{l+1}^\dagger b_l + b_l^\dagger b_{l+1}] + \epsilon_l n_l + \frac{U}{2} n_l(n_l - 1) \right), \quad (1)$$

where $n_l = b_l^\dagger b_l$. Here $\epsilon_l = h_l + bl^2$ includes a random on-site energy h_l and an axially confining harmonic potential, and J_l is a random hopping amplitude between neighboring sites. In optical lattices, hopping disorder is suppressed against on-site disorder [6], and we thus take $J_l \equiv J$, but h_l distributed according to a Gaussian ensemble [27] with

$$\overline{h_l} = 0, \quad \overline{h_l h_{l'}} = \Delta \delta_{ll'}, \quad (2)$$

where the overbar denotes the disorder average and Δ the disorder strength. Using the spatial diffusion constant D_s , for a given disorder mechanism, $\Delta = \hbar^2 v_F^3 / (a D_s)$ can be expressed in terms of microscopic parameters; v_F is defined after Eq. (7) below. Detailed theoretical estimates for D_s (and hence Δ) are available for laser speckle fields [4] and quasiperiodic optical lattices [5, 6], where also the Gaussian distribution of the disorder field h_l is justified. We show below that the neglect of disorder in the J_l is no fundamental restriction.

In the hard-core boson limit, $U \rightarrow \infty$, only the occupation numbers $n_l = 0$ or 1 are allowed, and then Eq. (1) can be mapped to a non-interacting lattice fermion model by means of a Jordan-Wigner transformation, $b_l = e^{i\pi \sum_{j < l} c_j^\dagger c_j} c_l$, where the c_l denote lattice fermion operators. This transformation results in the fermionic Hamiltonian

$$H = \sum_l \left(-J_l [c_{l+1}^\dagger c_l + c_l^\dagger c_{l+1}] + \epsilon_l c_l^\dagger c_l \right). \quad (3)$$

It provides a one-to-one mapping, preserving the Hilbert space structure of the bosonic problem, with the N -particle bosonic wavefunction expressed in terms of the fermionic one as [16]

$$\Phi_\nu^B(l_1, \dots, l_N) = |\Phi_\nu^F(l_1, \dots, l_N)|. \quad (4)$$

The energy level E_ν for an N -boson eigenstate Φ_ν^B can thereby be computed in terms of the non-interacting fermionic Hamiltonian (3). In particular, with the single-particle energy $\epsilon_i^{(j)}$ for the j th fermion residing in a single-particle solution Ψ_i to Eq. (3), and taking into account the exclusion principle, $E_\nu = \sum_{j=1}^N \epsilon_i^{(j)}$. The

many-body fermionic wavefunction $\Phi_\nu^F(l_1, \dots, l_N)$, and hence also the bosonic one (up to a sign), is then a Slater determinant, $\det[\Psi_i(l_j)]/\sqrt{N!}$. Since the modulus square does not change under the mapping (4), all bosonic quantities given solely in terms of $|\Phi_\nu^B|^2$ coincide with the fermionic ones. This includes all correlation functions of the particle density and the local density of states (LDoS),

$$\rho(\epsilon, l) = \sum_\nu \sum_{l_2, \dots, l_N} \delta(\epsilon - E_\nu) |\Phi_\nu^B(l, l_2, \dots, l_N)|^2.$$

The density of states (DoS) per site in a lattice with L sites is then $\rho(\epsilon) = \sum_{l=1}^L \rho(\epsilon, l)/L$, and also remains invariant. The same reasoning applies to the continuum limit studied later. In particular, the compressibility κ , and thus also the sound velocity, is simply

$$\kappa^{-1} = \frac{\pi^2}{m} \left(\frac{N}{La} \right)^3, \quad (5)$$

where m is the atomic mass. We set $\hbar = 1$ and temperature to zero from now on.

The equality of fermionic and bosonic results does not apply to the momentum distribution,

$$\overline{\hat{n}(p)} = \frac{1}{N} \sum_{ll'} e^{-ip(l-l')a} \overline{\langle b_l^\dagger b_{l'} \rangle}. \quad (6)$$

Nevertheless, the Bose-Fermi mapping allows for a rather simple exact calculation of the disorder-averaged boson momentum distribution. Using the Jordan-Wigner transformation and Wick's theorem, Eq. (6) for a given disorder realization can be written as a Töplitz determinant. For $l > l'$, we find $\langle b_l^\dagger b_{l'} \rangle = 2^{l-l'-1} \det[G^{(l,l')}]$, where the $(l-l') \times (l-l')$ matrix has the entries $G_{i,j}^{(l,l')} = \langle c_{l'+i}^\dagger c_{l'+j-1} \rangle - \delta_{i,j-1}/2$, see also Ref. [23]. For fixed disorder $\{h_l\}$ and arbitrary trap potential, we compute Eq. (6) numerically and subsequently average over different disorder realizations. This is a much faster and more reliable procedure than directly studying interacting dirty bosons [12, 14], since we have to deal with a single-particle problem only. Let us first consider ^{87}Rb atoms in a harmonic axial trap with $b = 0.01J$, see Eq. (1). The overall energy scale is set by J , which can be tuned in optical lattices over a wide range [23]. We show results for $N = 50$ atoms in Figure 1. Clearly, disorder has a significant effect on the momentum distribution. In particular, some weight is transferred to large momenta, and the zero-momentum peak decreases, see inset in Fig. 1. The momentum distribution has already been measured for bosonic atoms in the clean 1D limit using Bragg spectroscopy [28], and through imaging of the atom cloud after sudden removal of the trap potential [23]. Applying these techniques to the disordered case would allow to test our predictions. Note that these changes in the momentum distribution reflect Anderson localization physics, and should differ even qualitatively in the small- U limit.

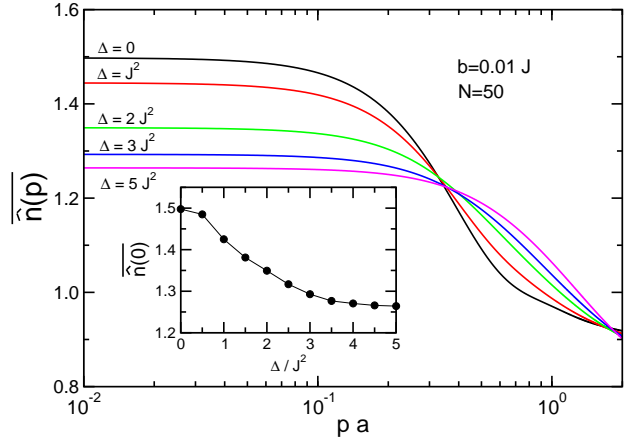


FIG. 1: (Color online) Momentum distribution (6) for several Δ and $N = 50$ rubidium atoms in a harmonic axial trap. For the disorder average, at most 300 disorder realizations were sufficient for convergence, and L was chosen large enough to ensure L -independence. Note the linear-logarithmic scale. Inset: Zero-momentum peak as a function of disorder strength.

For a clean homogeneous ($b = 0$) system, the boson momentum distribution is well-known to possess a $\hat{n}(p \rightarrow 0) \propto |p|^{-1/2}$ singularity [18, 19], corresponding to the one-particle density matrix $\rho(x, x') \propto |x - x'|^{-1/2}$ for $|x - x'| \rightarrow \infty$. In the thermodynamic limit, Bose-Einstein condensation is absent, but there is quasi-long-range order characterized by the $p^{-1/2}$ law. Remarkably, disorder has a fundamental effect on this singular behavior. The reasoning of Ref. [29] allows to prove that $\hat{n}(0)$ now must remain finite. The full momentum distribution $\overline{\hat{n}(p)}$ is obtained numerically and shown for a ring with periodic boundary conditions in Fig. 2. The complete destruction of quasi-long-range order by disorder is clearly visible, and the momentum distribution becomes remarkably flat for sufficiently strong disorder.

The Bose-Fermi mapping can also be established via the low-energy theory [13], which is a perhaps more natural description for magnetically trapped or micro-chip confined atoms, where no underlying lattice is present [7]. Focussing on circular or hard-wall axial trap potentials ($b = 0$), corresponding to periodic or open boundary conditions, the resulting fermionic theory coincides with the continuum limit ($a \rightarrow 0$) of Eq. (3). For a generic incommensurate filling N/L , we decompose the operator c_l into right- and left-moving (ψ_R, ψ_L) components with momenta $k \approx \pm k_F \equiv \pm \pi N/La$ according to $c_l \simeq \sqrt{a} [e^{ik_F x} \psi_R(x) + e^{-ik_F x} \psi_L(x)]$, where $x = la$. Correspondingly, the random on-site energies h_l can be decomposed into a slow part and a term varying on a microscopic scale, $h_l \approx \mu(x) + (\xi(x)e^{-i2k_F x} + \text{h.c.})$. For $h_l = 0$, we have a 1D massless Dirac Hamiltonian, $\xi(x)$ produces a complex-valued random mass term, and $\mu(x)$ a random chemical potential. Additional disorder in the J_l can be included in $\mu(x)$ and $\xi(x)$, and with bispinor $\psi = (\psi_R, \psi_L)$, the continuum model reads

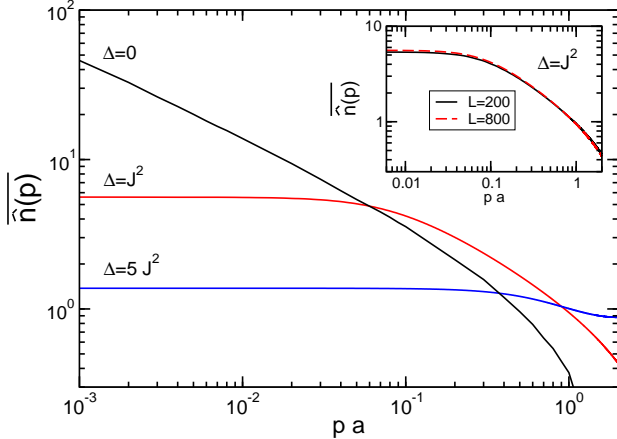


FIG. 2: (Color online) Momentum distribution on a ring for various Δ , $N/L = 1/2$, with $L = 600$. The $\Delta = 0$ result is analytical [18, 19] and shows the $p^{-1/2}$ scaling at $p \rightarrow 0$. Note the double-logarithmic scale. The inset shows that for finite Δ and $L \geq 200$, finite-size effects are negligible.

$H = \int dx \psi^\dagger \hat{h} \psi$ with

$$\hat{h} = -iv_F \sigma^z \partial_x + \mu(x) + \xi(x) \sigma^+ + \xi^*(x) \sigma^-, \quad (7)$$

where $v_F = 2aJ \sin(k_F a)$ is the Fermi velocity. Here the 2×2 matrices $\sigma^\pm = (\sigma^x \pm i\sigma^y)/2$ are defined in terms of Pauli matrices σ^i acting in spinor space. Equation (7) is the standard non-interacting Hamiltonian used to study Anderson localization in 1D conductors [27, 30, 31, 32]. The forward scattering term $\mu(x)$ can be eliminated by a gauge transformation and does not affect the quantities of interest below. (This is not possible on half-filling, where $\xi(x)$ is real-valued and important differences arise [27].) Equation (2) then implies

$$\overline{\xi(x)} = \overline{\xi^*(x)} = 0, \quad \overline{\xi^*(x)\xi(x')} = \frac{v_F}{2\tau} \delta(x - x'), \quad (8)$$

with $\tau = \ell/v_F$ for mean free path ℓ , which also gives the localization length. We only discuss weak disorder, $k_F \ell \gg 1$, where the bosonic system is in the Bose glass phase [1, 13]. The average DoS is simply $\bar{\rho}(\epsilon) = 1/(\pi v_F)$ [27], and we turn to the LDoS probability distribution.

The bosonic LDoS (from now on normalized to the average DoS) can be expressed in terms of eigenstates $\Psi_i(x)$ with energy ϵ_i of the Hamiltonian (7), $\rho(\epsilon, x) = \pi v_F \sum_i |\Psi_i(x)|^2 \delta(\epsilon - \epsilon_i)$. In a finite and closed sample, these levels are discrete and sharp, and it is necessary to regularize the δ -functions. A natural way [31] is to smear out the δ -peaks, $\rho_f(\epsilon, x) = \int d\epsilon' \rho(\epsilon', x) f(\epsilon - \epsilon')$, for instance by using a Lorentzian weight function, $f_\eta(\epsilon) = \eta/(\pi[\epsilon^2 + \eta^2])$. Physically, the width η is determined by inelastic processes, finite sample lifetimes, and escape rates of the trap. For an infinite sample, ρ_f then follows the inverse Gaussian probability distribution [31]

$$W(\rho_f) = \sqrt{\frac{4\eta\tau}{\pi\rho_f^3}} e^{-4\eta\tau(\rho_f - 1)^2/\rho_f}, \quad (9)$$

which decreases exponentially both as a function of ρ_f for $\rho_f \rightarrow \infty$, and as a function of $1/\rho_f$ for $\rho_f \rightarrow 0$. The anomalously small probability to find small ρ_f implies a Poisson distribution of the energy levels, indicating the absence of correlations among close-by levels. This is obvious in the fermionic picture, where energy levels of localized non-overlapping states cannot repel each other. In the strongly interacting bosonic picture, where well-defined single-particle states need not exist, this is a much less obvious result. Let us average $\rho_f(\epsilon, x)$ also over a spatial range δ determined by the spatial resolution, e.g., the wavelength of a probe laser. For $1/k_F \ll \delta \ll \ell$ and $4\eta\tau \ll 1$, the resulting LDoS $\tilde{\rho}(\epsilon, x)$ is independent of δ and follows the distribution [31]

$$\tilde{W}(\tilde{\rho}) = \frac{\eta\tau}{\pi} \int_4^\infty dt t \sin(\pi\eta\tau t) \left(\frac{t+4}{t-4} \right)^{\eta\tau t} e^{-\frac{1}{2}\eta\tau\tilde{\rho}t^2}, \quad (10)$$

which is a somewhat narrower distribution than $W(\rho_f)$. Both Eqs. (9) and (10) remain valid also in a finite closed sample, as long as the distance to any boundary is large compared to ℓ . The LDoS can be measured using imaging methods or two-photon Bragg spectroscopy [33, 34], thus allowing for experimental checks.

We then briefly discuss the bosonic LDoS correlations $R(\omega, x)$ at different energies and locations,

$$R(\omega, x - x') = \overline{\tilde{\rho}(\epsilon, x)\tilde{\rho}(\epsilon + \omega, x')} - 1, \quad (11)$$

which equal the fermionic ones computed in Ref. [30]. The correlator (11) describes fluctuations in the spectral statistics related to energy level repulsion or attraction. It is translationally invariant and independent of the energy ϵ after the disorder average [32]. Since $R(\omega, x = x') = 0$ [30, 31, 35], we consider $k_F|x - x'| \gg 1$ and $\omega\tau \ll 1$, where the correlator (11) is finite, with the limiting values $R = -1/3$ for small x and $R = 0$ for $x \rightarrow \infty$. In addition, there is a deep dip for $\ell \ll x \ll z_0(\omega) = 2\ell \ln(8/\omega\tau)$, where

$$R(\omega, \ell \ll x \ll z_0) = -1 + \frac{\pi^{7/2} e^{-x/4\ell}}{16(x/\ell)^{3/2}}. \quad (12)$$

Here $z_0(\omega)$ is the distance two nearly degenerate localized states must have to generate the energy splitting ω . The dip (12) implies that two states with nearly equal energies occupy with high probability locations far away from each other. Nevertheless, the wavefunctions of these states must have an appreciable overlap for short distances, $x \lesssim \ell$. For $x \gtrsim z_0$, the LDoS correlations approach the uncorrelated limit,

$$R(\omega, x \gtrsim z_0) = \frac{1}{2} \left[\text{erf} \left(\frac{x - z_0}{2\sqrt{z_0\ell}} \right) - 1 \right], \quad (13)$$

where $\text{erf}(x)$ denotes the error function. These features illustrate that the localized states are centered on many defects, leading to a complicated quantum interference phenomenon. As a consequence, close-lying levels do not

obey the usual Wigner-Dyson spectral correlations found in granular metals [32], but instead follow the Poisson statistics of uncorrelated energy levels. It would obviously be quite exciting to probe (11) experimentally. For ultracold bosonic atoms, this is possible using stimulated two-photon Bragg scattering spectroscopy [33]. Similarly, one can compute the (Fourier-transformed) bosonic density-density correlations $K(x - x', \omega)$,

$$\text{Re } K(x, \omega + i0) = \pi \int d\epsilon n_F(\epsilon) [1 - n_F(\epsilon + \omega)] p(x; \epsilon + \omega, \epsilon), \quad (14)$$

where $n_F(\epsilon)$ is the Fermi function, and the fermionic spectral function

$$p(x - x'; \epsilon + \omega, \epsilon) = \frac{\sum_{ij} \delta(\epsilon + \omega - \epsilon_i) \delta(\epsilon - \epsilon_j) \Psi_i(x) \Psi_i^*(x') \Psi_j^*(x') \Psi_j(x)}{\sum_{ij} \delta(\epsilon + \omega - \epsilon_i) \delta(\epsilon - \epsilon_j)}$$

is a phase-sensitive quantity without a direct bosonic image. This nicely illustrates that the Bose-Fermi mapping opens otherwise unavailable routes for calculation. For $x \gtrsim z_0$ [30],

$$p(x; \epsilon + \omega, \epsilon) = -\frac{\exp\left[-\frac{(x-z_0)^2}{4z_0\ell}\right]}{2(\pi v_F)^2 \sqrt{\pi z_0/\ell}}, \quad (15)$$

while for $x \lesssim z_0$, to very good approximation [30], $p(x; \epsilon + \omega, \epsilon) = (\pi v_F)^{-2}(R(\omega, x) + 1)$.

To conclude, we have provided exact results for strongly repulsive dirty bosons in 1D, which can be obtained from a Bose-Fermi mapping to non-interacting disordered fermions. A Bose-glass phase is thereby mapped to an Anderson-localized fermionic phase. A similar mapping is also available for arbitrary interaction strength, but involves interacting fermions with a non-standard contact interaction [36]. For strong (but finite) repulsive bosonic interactions, the weak fermionic interactions can safely be treated on a perturbative level [13] and cause no substantial differences to our predictions. Finally, other quantities not discussed here can also be inferred, e.g., the crossover from short-time diffusive wave-packet expansion to localized behavior at long times [35].

We thank A. Görlitz and A.O. Gogolin for discussions. This work was supported by the SFB TR/12 of the DFG.

-
- [1] M.P.A. Fisher, P.B. Weichman, G. Grinstein, and D.S. Fisher, Phys. Rev. B **40**, 546 (1989).
 - [2] D. Jaksch, C. Bruder, J.I. Cirac, C.W. Gardiner, and P. Zoller, Phys. Rev. Lett. **81**, 3108 (1998).
 - [3] M. Greiner, O. Mandel, T. Esslinger, T.W. Hänsch, and I. Bloch, Nature **415**, 39 (2002).
 - [4] P. Horak, J.-Y. Courtois, and G. Grynberg, Phys. Rev. A **58**, 3953 (2000).
 - [5] A. Sanpera, A. Kantian, L. Sanchez-Palencia, J. Zakrzewski, and M. Lewenstein, Phys. Rev. Lett. **93**, 040401 (2004).
 - [6] B. Damski, J. Zakrzewski, L. Santos, P. Zoller, and M. Lewenstein, Phys. Rev. Lett. **91**, 080403 (2003).
 - [7] R. Folman, P. Krüger, J. Schmiedmayer, J. Denschlag, and C. Henkel, Adv. At. Mol. Opt. Phys. **48**, 263 (2002).
 - [8] L. Zhang and M. Ma, Phys. Rev. B **45**, 4855 (1992).
 - [9] R.T. Scalettar, G.G. Batrouni, and G.T. Zimanyi, Phys. Rev. Lett. **66**, 3144 (1991).
 - [10] K.G. Singh and D.S. Rokhsar, Phys. Rev. B **46**, 3002 (1992).
 - [11] A.V. Lopatin and V.M. Vinokur, Phys. Rev. Lett. **88**, 235503 (2002).
 - [12] N. Prokof'ev and B. Svistunov, Phys. Rev. Lett. **92**, 015703 (2004).
 - [13] T. Giamarchi and H.J. Schulz, Europhys. Lett. **3**, 1287 (1987); Phys. Rev. B **37**, 325 (1988).
 - [14] S. Rapsch, U. Schollwöck, and W. Zwerger, Europhys. Lett. **46**, 559 (1999).
 - [15] L. Tonks, Phys. Rev. **50**, 955 (1936).
 - [16] M. Girardeau, J. Math. Phys. **1**, 516 (1960).
 - [17] E.H. Lieb and W. Liniger, Phys. Rev. **130**, 1605 (1963).
 - [18] A. Lenard, J. Math. Phys. **5**, 930 (1964).
 - [19] H.G. Vaidya and C.A. Tracy, Phys. Rev. Lett. **42**, 3 (1979). See also D.M. Gangardt, J. Phys. A: Math. Gen. **37**, 9335 (2004).
 - [20] F.D.M. Haldane, Phys. Rev. Lett. **47**, 1840 (1981).
 - [21] D.S. Petrov, G.V. Shlyapnikov, and J.T.M. Walraven, Phys. Rev. Lett. **85**, 3745 (2000).
 - [22] V. Dunjko, V. Lorent, and M. Olshanii, Phys. Rev. Lett. **86**, 5413 (2001).
 - [23] B. Paredes et al., Nature **429**, 277 (2004).
 - [24] T. Kinoshita, T. Wenger, and D.S. Weiss, Science **305**, 112 (2004).
 - [25] A. Görlitz et al., Phys. Rev. Lett. **87**, 130402 (2001).
 - [26] H. Moritz, T. Stöferle, M. Köhl, and T. Esslinger, Phys. Rev. Lett. **91**, 250402 (2003).
 - [27] I.M. Lifshits, S.A. Gredeskul, and L.A. Pastur, *Introduction to the theory of disordered systems* (John Wiley & Sons, New York, 1988).
 - [28] S. Richard et al., Phys. Rev. Lett. **91**, 010405 (2003).
 - [29] A. Klein and J.F. Perez, Comm. Math. Phys. **128**, 99 (1990).
 - [30] L.P. Gor'kov, O.N. Dorokhov, and F.V. Prigara, Zh. Eksp. Teor. Fiz. **84**, 1440 (1983) [Sov. Phys. JETP **57**, 838 (1983)]; Zh. Eksp. Teor. Fiz. **85**, 1470 (1983) [Sov. Phys. JETP **58**, 852 (1983)].
 - [31] B.L. Al'tshuler and V.N. Prigodin, Zh. Eksp. Teor. Fiz. **95**, 348 (1989) [Sov. Phys. JETP **68**, 198 (1989)].
 - [32] K.B. Efetov, *Supersymmetry in disorder and chaos* (Cambridge University Press, 1997).
 - [33] J. Stenger et al., Phys. Rev. Lett. **82**, 4569 (1999).
 - [34] T. Stöferle, H. Moritz, C. Schori, M. Köhl, and T.

- Esslinger, Phys. Rev. Lett. **92**, 130403 (2004).
- [35] E.P. Nachmedov, V.N. Prigodin, and Yu.A. Firsov, Zh. Eksp. Teor. Fiz. **92**, 2133 (1987) [Sov. Phys. JETP **65**, 1202 (1987)].
- [36] T. Cheon and T. Shigehara, Phys. Rev. Lett. **82**, 2536 (1999).